

## Strand Invasion of Extended, Mixed-Sequence B-DNA by $\gamma$ PNAs

Gaofei He, Srinivas Rapireddy, Raman Bahal, Bichismita Sahu, and Danith H. Ly\*

Department of Chemistry and Center for Nucleic Acids Science and Technology (CNAST), Carnegie Mellon University, 4400 Fifth Avenue, Pittsburgh, Pennsylvania 15213

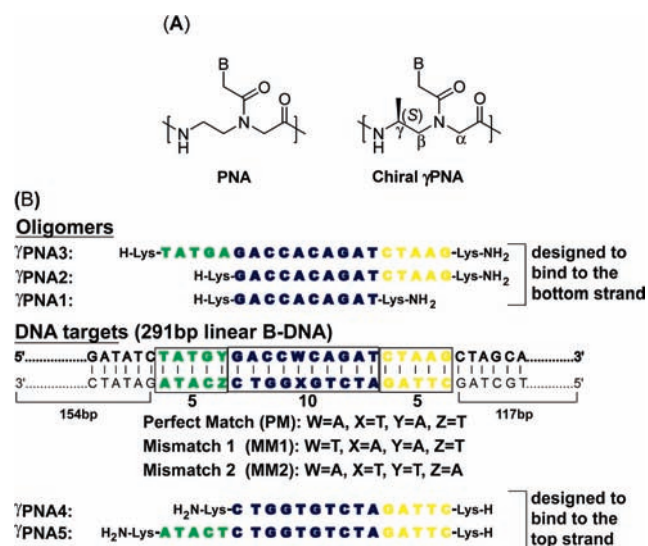
Received January 12, 2009; E-mail: dly@andrew.cmu.edu

Peptide nucleic acids (PNAs) are a promising class of nucleic acid mimics developed in the last two decades in which the naturally occurring sugar phosphodiester backbone has been replaced by achiral *N*-(2-aminoethyl)glycine units (Scheme 1A).<sup>1</sup> In addition to their ability in hybridizing to cDNA or RNA strands, PNAs can invade double-stranded DNA.<sup>2</sup> Strand invasion occurs predominantly in two modes, depending on the target sequence: through Watson–Crick base pairing to form a 1:1 PNA/DNA complex<sup>3</sup> or in combination with Hoogsteen base pairing to form a 2:1 complex.<sup>4</sup> The simplicity and generality of their recognition along with the ease and flexibility of their synthesis make PNAs an attractive class of antigene reagents. However, with the current design, not every sequence can be accessed by PNAs; in particular, those that contain all four nucleobases are not accessible. Mixed-sequence PNAs have been shown to be capable of invading supercoiled plasmid DNA<sup>5–7</sup> and certain regions of genomic DNA,<sup>8</sup> but they are not capable of invading intact, linear double-helical B-form DNA (B-DNA). Recently, two approaches, “tail-clamp”<sup>9,10</sup> and “double-duplex”<sup>11</sup> invasion, that enable mixed-sequence PNAs to invade B-DNA have been developed. However, they are not without limitations. The first approach still requires a stretch of homopurine target for anchoring triplex binding, while the second, although more relaxed in sequence selection, requires an elaborate nucleobase substitution and the need to use two strands of PNAs to invade B-DNA, complicating their design and greatly limiting their utility.<sup>12</sup> In this communication, we show that mixed-sequence PNAs with lengths of 15–20 nucleotides (nt), when preorganized into a right-handed helix, can invade double-helical B-DNA. Strand invasion occurs in a sequence-specific manner through direct Watson–Crick base pairing. In this case, only a single strand of  $\gamma$ PNA is required for invasion, and no nucleobase substitution is needed.

Recently, we showed that PNAs, which as individual strands do not have well-defined conformations, can be preorganized into a right-handed helix by installing an (*S*)-Me stereogenic center at the  $\gamma$ -backbone position (Scheme 1A).<sup>13</sup> These helical  $\gamma$ PNAs exhibit strong binding affinity for cDNA and RNA strands. As decamers, mixed-sequence  $\gamma$ PNAs are unable to invade B-DNA, but strand invasion can be rescued by appending an acridine moiety (DNA intercalator) to one of the termini<sup>13</sup> or by replacing a cytosine nucleobase with an energetically more favorable synthetic analogue.<sup>14</sup> These results suggest that the binding free energies of the decameric  $\gamma$ PNAs are already near the invasion threshold and that not much more is needed to enable them to invade B-DNA. On the basis of these findings, we speculated that as an alternative to the aforementioned strategies, the required binding free energy may also be attained by extending the size of the  $\gamma$ PNA oligomers, since a  $\gamma$ PNA–DNA duplex is generally thermodynamically more stable than a DNA–DNA duplex. If this design strategy could be achieved, it would not only circumvent the need to attach ancillary agents to PNAs, which may compromise their recognition specificity and complicate their synthesis, but also allow  $\gamma$ PNAs to recognize

extended DNA targets, which has been a goal of antigene design.<sup>2,15,16</sup> To test this hypothesis, we synthesized a series of  $\gamma$ PNA oligomers with various sizes (Scheme 1B) that were designed to bind to both the top and bottom strands of the DNA target and then assessed their invasion capability using a combination of gel-shift, enzymatic, and chemical-probing assays.

**Scheme 1.** (A) Chemical Structures of PNA and  $\gamma$ PNA and (B) Sequence of  $\gamma$ PNAs and a Selected Region of the DNA Target



The gel-shift assay was performed by incubation of a 291 base pair (bp) PCR fragment containing a perfect-match (PM) binding site with different concentrations of  $\gamma$ PNA1–3 in 10 mM sodium phosphate (NaPi) buffer at 37 °C for 16 h, followed by gel separation and SYBR Gold staining. Consistent with our earlier result,<sup>13</sup> we observed no binding of  $\gamma$ PNA1, a decamer, at  $\gamma$ PNA/DNA ratios as high as 20:1 (Figure 1A, lanes 3 and 4). However, in the case of 15-mer  $\gamma$ PNA2 and 20-mer  $\gamma$ PNA3, we noticed the appearance of a shifted band (lanes 5, 6, 8 and 9). The intensity of the new band gradually increased with increasing  $\gamma$ PNA concentration, and the mobility decreased with increasing oligomer length. Formation of this complex appeared to be more efficient with  $\gamma$ PNA3 than with  $\gamma$ PNA2, as reflected in the ratio of the bound-to-unbound DNA (compare lanes 8 with 5 and lanes 9 with 6). This is expected, since  $\gamma$ PNA3 should form a thermodynamically more stable complex with DNA as a result of its greater length. Binding appeared to be unique to  $\gamma$ PNAs and occurred in a sequence-specific manner: neither incubation of DNA containing the PM binding site with PNAs having identical nucleobase sequences (PNA2, lane 7; PNA3, lane 10) nor incubation of DNA having a single-base mismatch in the middle (MM1) or toward one end (MM2) of the binding site with  $\gamma$ PNAs resulted in formation of any shifted bands (Figure 1B, lanes 4–9). Similar findings were

also observed with 15-mer  $\gamma$ PNA4 and 20-mer  $\gamma$ PNA5, which were designed to bind to the top strand of the DNA target (Figure 2). Formation of the retarded band was observed only with **PM** (lanes 1–8) and not with **MM1** (lane 9) or **MM2** (lane 10). However, when an equimolar ratio of  $\gamma$ PNA3 and  $\gamma$ PNA5 was added, no retarded band was observed (lane 8). This was expected, since the two  $\gamma$ PNA strands are complementary to one another and thus should hybridize to each other rather than invade the DNA double helix, as a  $\gamma$ PNA– $\gamma$ PNA duplex is thermodynamically more stable than a  $\gamma$ PNA–DNA duplex. A time-course study revealed that formation of this complex reached equilibrium within  $\sim 8$  h of incubation and followed pseudo-first-order kinetics (Figure 3).

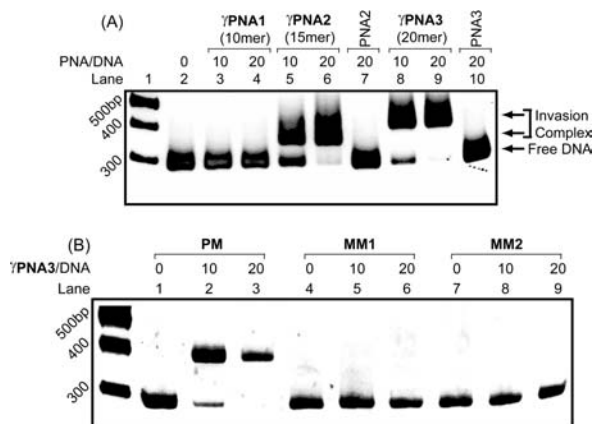


**Figure 1.** Gel-shift assay following incubation of  $0.1 \mu\text{M}$  291 bp DNA fragments containing various binding sites with PNAs and  $\gamma$ PNAs: (A) **PM** binding site with different concentrations of  $\gamma$ PNAs (lanes 3–6, 8, and 9) and PNAs (lanes 7 and 10); (B) **PM** (lanes 1–3), **MM1** (lanes 4–6), and **MM2** (lanes 7–9) binding sites with different concentrations of  $\gamma$ PNA3. Incubations were performed in 10 mM NaPi buffer at  $37^\circ\text{C}$  for 16 h and followed by nondenaturing PAGE separation and SYBR Gold staining. PNA2 and PNA3 contained the same nucleobase sequences as  $\gamma$ PNA2 and  $\gamma$ PNA3, respectively, but did not have  $\gamma$ -backbone modifications.

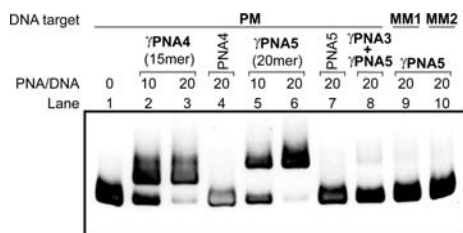


**Figure 2.** Gel-shift assay following incubation of  $0.1 \mu\text{M}$  PCR fragments containing **PM** (lanes 1–8), **MM1** (lane 9), and **MM2** (lane 10) binding sites with different concentrations of  $\gamma$ PNAs ( $\gamma$ PNA4, lanes 2 and 3;  $\gamma$ PNA5, lanes 5, 6, 9, and 10;  $\gamma$ PNA3 +  $\gamma$ PNA5, lane 8) and PNAs (PNA4, lane 4; PNA5, lane 7) under conditions identical to those in Figure 1.  $\gamma$ PNA4 and  $\gamma$ PNA5 were designed to bind to the top strand of the **PM**, **MM1**, and **MM2** targets;  $\gamma$ PNA3 and  $\gamma$ PNA5 are complementary to one another.

To confirm that these  $\gamma$ PNAs bind to their designated sites through a strand invasion mechanism, we performed S1 nuclease digestion where the 3' end of the homologous DNA strand was labeled with P-32. S1 nuclease was chosen because it is known to selectively cleave single-stranded DNA or melted regions of double-stranded DNA. Invasion of  $\gamma$ PNAs into the DNA double helix is expected to result in a local displacement of the homologous DNA strand, which can be revealed in the form of strand cleavage following S1 nuclease digestion. Figure 4 reveals the digestion patterns of 171 bp PCR fragments containing **PM** (lanes 1–8), **MM1** (lanes 9 and 10) and **MM2** (lanes 11 and 12) binding sites

following incubation with  $\gamma$ PNAs and PNA. Contrary to the gel-shift assay, where we did not observe any evidence of binding of  $\gamma$ PNA1, we observed cleavage of the homologous DNA strand directly across from its binding site (lanes 2 and 3). Because of the susceptibility of the homologous strand to S1 nuclease digestion, this result indicates that strand invasion did take place, so the fact that no retarded band was observed in the gel-shift assay indicates that the complex was not sufficiently stable to withstand the prolonged electrophoresis. Similar cleavage patterns were observed for  $\gamma$ PNA2 and  $\gamma$ PNA3, but they were more extensive in coverage, roughly five bases further toward the 3' end for  $\gamma$ PNA2 (lanes 4 and 5) and five to eight bases further toward both the 3' and 5' ends for  $\gamma$ PNA3 (lanes 6 and 7). This was expected on the basis of their recognition coverage. No strand cleavage was observed with unmodified PNA3 (lane 8) or with  $\gamma$ PNA3 having mismatched targets (lanes 10 and 12). This result was further corroborated by diethyl pyrocarbonate (DEPC) chemical-probing assays,<sup>17,18</sup> which revealed selective cleavage of the homologous DNA strand at the adenine and, to a smaller extent, guanine residues across from their binding sites (Figures 1S and 2S). This was observed only with **PM** and not with the **MM1** or **MM2** binding site. These results are consistent with  $\gamma$ PNA binding through a strand invasion mechanism.

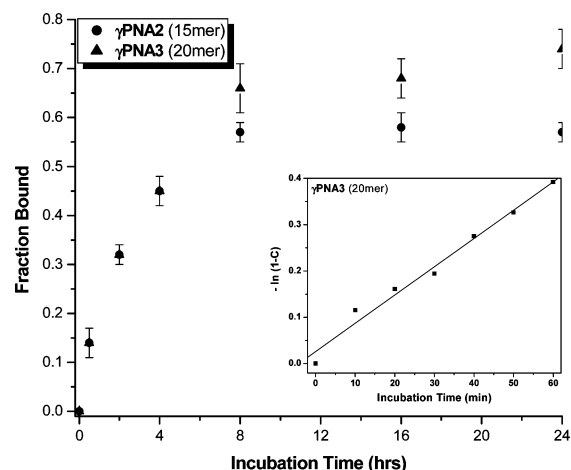


**Figure 3.** Time-dependent strand invasion of DNA by  $\gamma$ PNA2 and  $\gamma$ PNA3. The 291 bp PCR fragment with the **PM** binding site ( $0.1 \mu\text{M}$ ) was incubated with each  $\gamma$ PNA oligomer ( $1.0 \mu\text{M}$ ) in 10 mM NaPi at  $37^\circ\text{C}$  for the indicated periods. The mixtures were separated by nondenaturing PAGE and stained with SYBR Gold. The amounts of bound and unbound DNA were quantified by ImageJ software.

Further, we show that  $\gamma$ PNAs can be used to selectively inhibit restriction enzyme digestion. Incubation of a 321 bp DNA target containing the **PM** binding site with *Bgl II* resulted in two DNA fragments with lengths of 142 and 175 bp (Figure 5A,B, lane 3). When the DNA target was first incubated with  $\gamma$ PNA3 prior to addition of enzyme, the digestion was progressively more inhibited with increasing  $\gamma$ PNA3 concentration (lanes 4 and 5). This result indicates one of two possibilities: either  $\gamma$ PNA3 was bound to its target and thereby blocked the enzyme from cleaving the DNA at its restriction site, or  $\gamma$ PNA3 “poisoned” the enzyme through nonspecific binding. We ruled out the latter possibility on the basis of the mismatch result. When the DNA fragments containing **MM1** and **MM2** binding sites were used, no apparent inhibition of the restriction enzyme digestion was observed (lanes 7 and 9), indicating that the presence of  $\gamma$ PNA3 had no effect on the activity of *Bgl II*. This result shows that  $\gamma$ PNAs can be used as molecular tools to selectively manipulate the structure of B-DNA<sup>19</sup> and possibly other

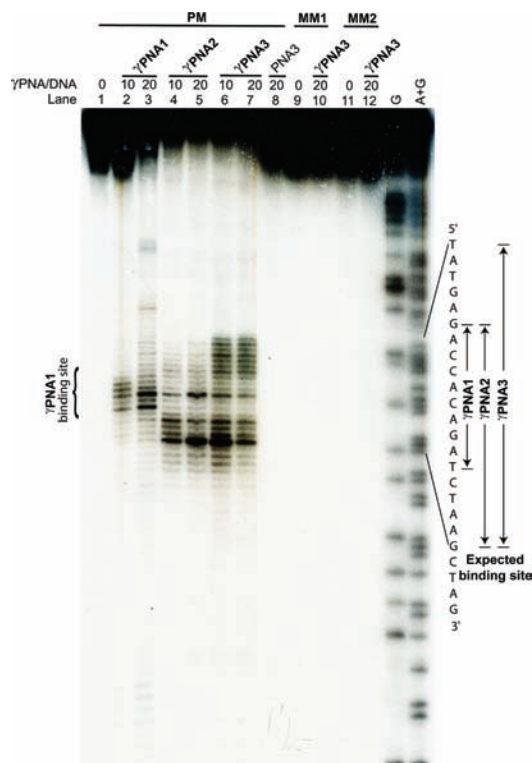


**Figure 4.** S1 nuclease digestion of 171 bp linear B-DNAs with **PM** (lanes 1–8), **MM1** (lanes 9 and 10), and **MM2** (lanes 11 and 12) binding sites following incubation with  $\gamma$ PNAs and PNA at the indicated ratios in 10 mM NaPi buffer at 37 °C for 16 h. The mixtures were reconstituted with 1  $\times$  S1 nuclease buffer [30 mM NaOAc and 1 mM Zn(OAc)<sub>2</sub>], treated with S1 nuclease (10 units for 20 min at room temperature), and finally separated on denaturing gel and imaged by autoradiography. The 3' end of the homologous DNA strand was labeled with P-32 using a Klenow fragment.

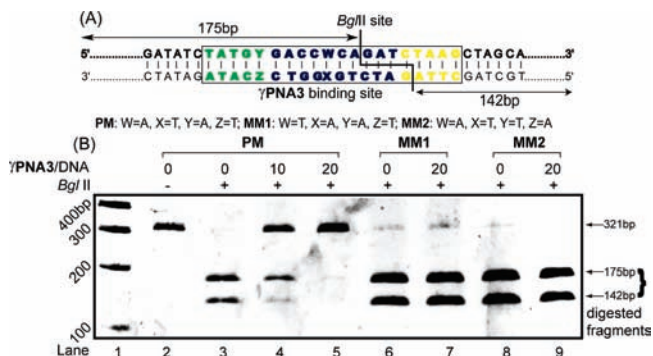


**Figure 5.** Restriction enzyme digestion of 321 bp PCR fragments containing **PM**, **MM1**, and **MM2** binding sites with  $\gamma$ PNA3. (A) Schematic diagram showing the *Bgl* II restriction and  $\gamma$ PNA3 binding sites along with the size of the predicted DNA fragments following *Bgl* II digestion. (B) Restriction digestion patterns of the DNA targets containing **PM** (lanes 2–5), **MM1** (lanes 6 and 7), and **MM2** (lanes 8 and 9) binding sites without (lanes 3, 6, and 8) and with (lanes 4, 5, 7, and 9) prior incubation with  $\gamma$ PNA3. Enzyme digestion was progressively inhibited in the presence of **PM** (lanes 4 and 5) but not with **MM1** (lane 7) or **MM2** (lane 9).

genome-sensing applications as well.<sup>20</sup> Once formed, the invasion complex remained stable over a prolonged period even at a relatively high ionic strength, as demonstrated in this study.

In summary, we have shown that mixed-sequence PNAs with lengths of 15–20 nt, when preorganized into a right-handed helix by installation of an appropriate stereogenic center on the  $\gamma$ -backbone, can invade double-helical B-DNA. We attribute the improvements in the ability of  $\gamma$ PNAs to invade B-DNA to their preorganized structure. This structure allows them to intercept the nucleobase targets more rapidly and stabilize the invasion complex more effectively than their achiral counterparts, since minimal structural rearrangement is required prior or subsequent to invasion. The results reported herein are important because they demonstrate that the same Watson–Crick base-pairing principles that guide the recognition of single-stranded DNA and RNA can also be applied to intact double-helical B-DNA. Recognition, in this case, is general to all four nucleobases and extended target sizes that may be difficult to achieve with other classes of molecules.<sup>16,21–23</sup>

**Acknowledgment.** Funding was provided in part by the National Institutes of Health to D.H.L. (GM076251).

**Supporting Information Available:** Sequences of DNA, PNA, and  $\gamma$ PNA oligomers; UV-melting transition temperatures; and DEPC assay results. This material is available free of charge via the Internet at <http://pubs.acs.org>.

**References**

- (1) Nielsen, P. E.; Egholm, M.; Berg, R. H.; Buchardt, O. *Science* **1991**, *254*, 1497.
- (2) Nielsen, P. E. *Acc. Chem. Res.* **1999**, *32*, 624.
- (3) Nielsen, P. E.; Christensen, L. *J. Am. Chem. Soc.* **1996**, *118*, 2287.
- (4) Egholm, M.; Nielsen, P. E.; Buchardt, O.; Berg, R. H. *J. Am. Chem. Soc.* **1992**, *114*, 9677.
- (5) Bentin, T.; Nielsen, P. E. *Biochemistry* **1996**, *35*, 8863.
- (6) Smulevitch, S. V.; Simmons, C. G.; Norton, J. C.; Wise, T. W.; Corey, D. R. *Nat. Biotechnol.* **1996**, *14*, 1700.
- (7) Zhang, X.; Ishihara, T.; Corey, D. R. *Nucleic Acids Res.* **2000**, *28*, 3332.
- (8) Janowski, B. A.; Kaihatsu, K.; Huffman, K. E.; Schwartz, J. C.; Ram, R.; Hardy, D.; Mendelson, C. R.; Corey, D. R. *Nat. Chem. Biol.* **2005**, *1*, 210.
- (9) Bentin, T.; Larsen, H. J.; Nielsen, P. E. *Biochemistry* **2003**, *42*, 13987.
- (10) Kaihatsu, K.; Shah, R. H.; Zhao, X.; Corey, D. R. *Biochemistry* **2003**, *42*, 13996.
- (11) Lohse, J.; Dahl, O.; Nielsen, P. E. *Proc. Natl. Acad. Sci. U.S.A.* **1999**, *96*, 11804.
- (12) Demidov, V. V.; Protozanova, E.; Izvol'sky, K. I.; Price, C.; Nielsen, P. E.; Frank-Kamenetskii, M. D. *Proc. Natl. Acad. Sci. U.S.A.* **2002**, *99*, 5953.
- (13) Rapireddy, S.; He, G.; Roy, S.; Armitage, B. A.; Ly, D. H. *J. Am. Chem. Soc.* **2007**, *129*, 15596.
- (14) Chenna, V.; Rapireddy, S.; Sahu, B.; Ausin, C.; Pedroso, E.; Ly, D. H. *ChemBioChem* **2008**, *9*, 2388.
- (15) Weyermann, P.; Dervan, P. B. *J. Am. Chem. Soc.* **2002**, *124*, 6872.
- (16) Jantz, D.; Amann, B. T.; Gatto, G. J.; Berg, J. M. *Chem. Rev.* **2004**, *104*, 789.
- (17) Scholten, P. M.; Nordheim, A. *Nucleic Acids Res.* **1986**, *14*, 3981.
- (18) Furlong, J. C.; Lilley, D. M. *J. Nucleic Acids Res.* **1986**, *14*, 3995.
- (19) Komiyama, M.; Aiba, Y.; Yamamoto, Y.; Sumaoka, J. *Nat. Protoc.* **2008**, *3*, 655.
- (20) Lin, J.; Lai, Z.; Aston, C.; Jing, J.; Anantharaman, T. S.; Mishra, B.; White, O.; Daly, M. J.; Minton, K. W.; Venter, J. C.; Schwartz, D. C. *Science* **1999**, *285*, 1558.
- (21) Gowers, D. M.; Fox, K. R. *Nucleic Acids Res.* **1999**, *27*, 1569.
- (22) Kelly, J. J.; Baird, E. E.; Dervan, P. B. *Proc. Natl. Acad. Sci. U.S.A.* **1996**, *93*, 6981.
- (23) Kielkopf, C. L.; Baird, E. E.; Dervan, P. B.; Rees, D. C. *Nat. Struct. Biol.* **1998**, *5*, 104.

JA900228J